CHAPTER – 5

Synthesis and Characterization of Zn- substituted Magnetite Nanoparticles

5.1 Introduction

It has been described in the last two chapters (Chapters 3 and 4) that the T_S near 42 - 46°C could be achieved by tetravalent (Zr or Hf) or trivalent (Al) substituted Fe_3O_4 nanoparticles in the presence of various AC magnetic fields. To the best of my knowledge, there were no reports on attaining such T_S values using substituted magnetite nanoparticles. These observations create an interest to study the heating behaviour of the divalent ions substituted magnetite ($Zn_xFe_{3-x}O_4$, $0.01 \leq x \leq 0.8$) during MHT. These MNPs used for the investigation were also prepared by microwave refluxing method. Simultaneously, the structural, microstructural and magnetic behaviours were characterized by the usual techniques.

5.2 Zn substituted magnetite nanoparticles

5.2.1 XRD Study

The XRD patterns of $Zn_xFe_{3-x}O_4$ ($0.01 \leq x \leq 0.8$) samples after Rietveld refinement are shown in Fig. 5.2.1 which suggests about the single phase cubic spinel structure with space group Fd_3m. No additional impurity phase has been detected within the limit of observation in the XRD patterns. The observed peaks are indexed as (220), (311), (400), (422), (511), (440) and (533) which matched with spinel's structure of FCC phase. Figure 5.2.2 (a) shows the variation of lattice parameter as a function of Zn concentration in magnetite. The lattice parameter found to be increasing from 8.357 to 8.434 Å as the Zn^{2+} concentration increased from 0.01 to 0.8. The diffraction peaks in the XRD patterns found to be shifted towards lower angle sides with increased Zn substitution. Due to this, we can conclude that Zn^{2+} ions occupy the interstitial site (tetrahedral) of the spinel structure.

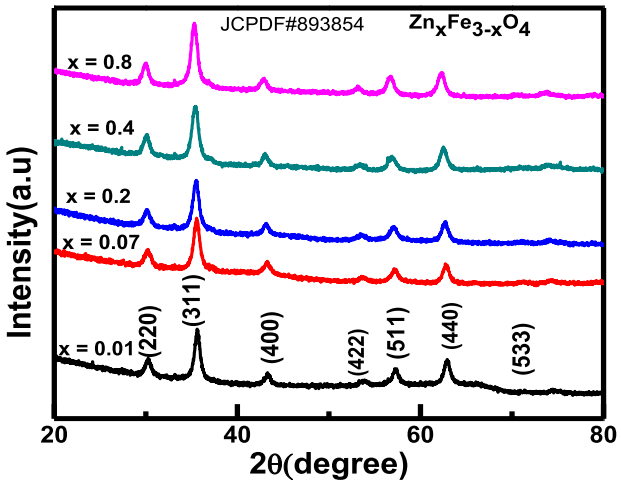

Fig. 5.2.1: XRD patterns of $Zn_xFe_{3-x}O_4$ (x = 0.01, 0.07, 0.2, 0.4 and 0.8) nanoparticles.

The earlier studies on Zn-substituted magnetites also suggest that Zn-ions will occupy at the tetrahedral sites only [74,75]. The occupancy of Zn-ions at tetrahedral voids are possible due their comparable ionic radii e.g. the radii at the tetrahedral site for Zn^{2+}, Fe^{2+} and Fe^{3+} are 0.74, 0.77 and 0.63 Å, respectively and at the octahedral site for Fe^{2+} and Fe^{3+} are 0.92 and 0.79 Å, respectively.

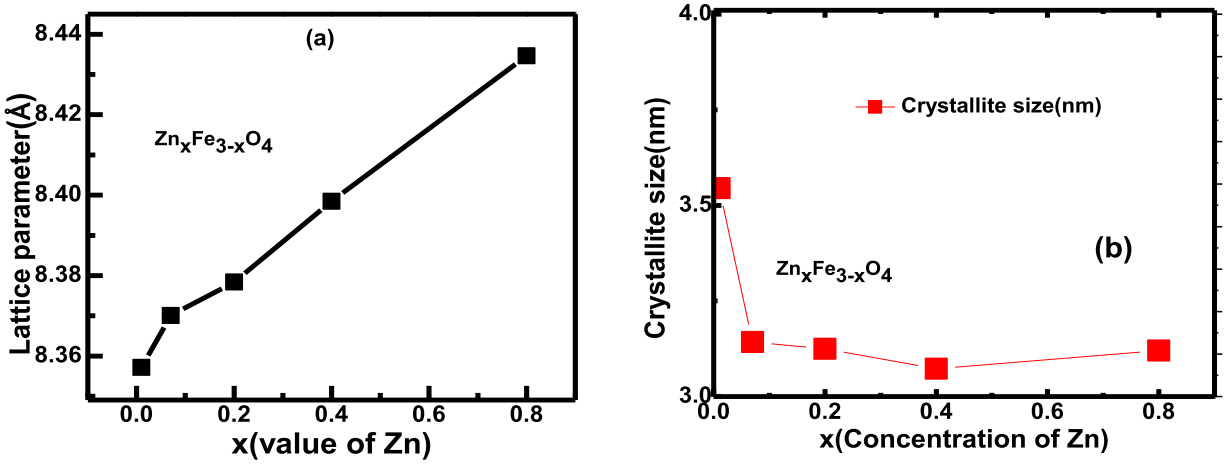

Fig.5.2.2: Variation with increased Zn content in (a) lattice parameter, (b) crystallite size.

The average crystallite size for $Zn_xFe_{3-x}O_4$ ($0.01 \leq x \leq 0.8$) samples was calculated using Scherer's formula. For the calculations, instrumental broadening was subtracted from the peak broadening. The crystallite size found to be decreasing continuously from ~ 4 (x = 0.01) to ~ 3nm (x = 0.8) with increased Zn concentration (Fig. 5.2.2 b).

5.2.2. TEM study

The bright field TEM micrographs of $Zn_{0.2}Fe_{2.8}O_4$ and $Zn_{0.8}Fe_{2.2}O_4$samples and the corresponding SAD patterns are shown in Fig. 5.2.3. The morphology of the as prepared samples found to be spherical in shape. The particles size was estimated by ImageJ software and found to be in the range of 3-11 nm. Selected area diffraction patterns confirmed the FCC phase that were similar to that of magnetite having inverse spinel structure (insets of Figs. 3a and b).

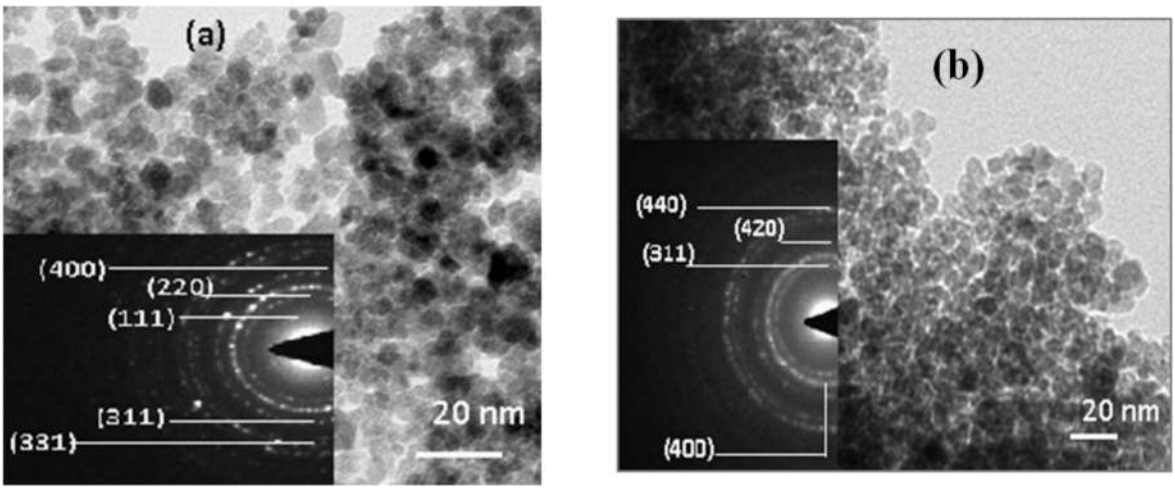

Fig. 5.2.3: TEM micrographs for (a) $Zn_{0.2}Fe_{2.8}O_4$ and (b) $Zn_{0.8}Fe_{2.2}O_4$ samples. Insets show corresponding SAD patterns.

5.2.3. XPS study

The X-ray photoelectron spectra of $Zn_{0.4}Fe_{2.6}O_4$ sample for Fe2p, Zn 2p, and O1s are shown in Fig. 5.2.4. The deconvolution of the Fe 2p core level spectrum contains two characteristic peaks for Fe^{3+} $2p_{3/2}$ and $2p_{1/2}$ at binding energies of 712.69 and 724.49 eV respectively [66]. The satellite peaks for Fe^{3+} were observed at 711.07 and 720.09 eV. In addition, the peaks for Fe^{2+} $2p_{3/2}$ and $2p_{1/2}$ were observed at binding energies 712 and 723.8 eV respectively. The characteristic peaks for Zn^{2+} $2p_{3/2}$ and $2p_{1/2}$ were noticed at 1021.2 and 1044.0 eV respectively[76]. Thus, the XPS study for the sample suggests that it contains Fe as Fe^{2+} and Fe^{3+} ions and Zn as Zn^{2+} ions.

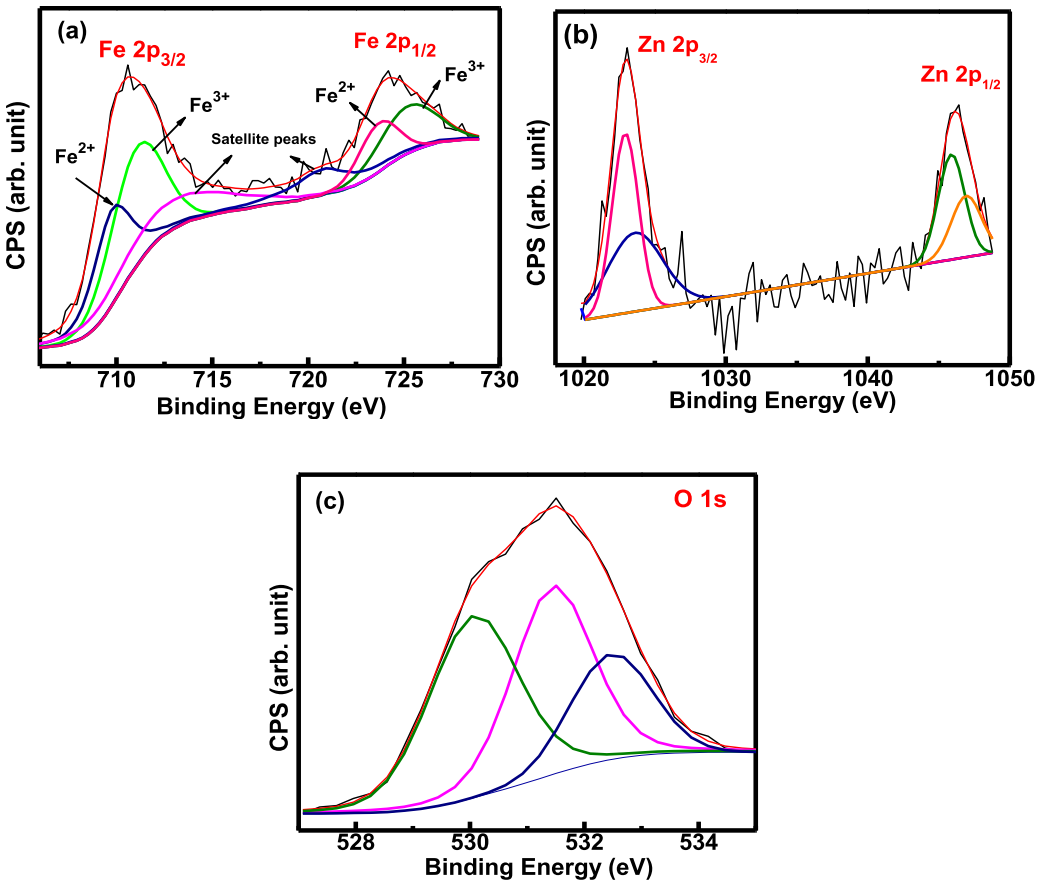

Fig. 5.2.4: XPS spectra of $Zn_{0.4}Fe_{2.6}O_4$ sample (a) Fe 2p (b) Zn2p and(c) O1s core level spectra.

5.2.4. Magnetization study

The magnetizations vs. field curves for $Zn_xFe_{3-x}O_4$ samples, which were measured at room temperature and up to ±2 T, are shown in Fig. 5.2.5 (a). There is slight initial increment in the M_S value which reaches to the maxima at x = 0.2 (i.e. 65 Am^2/kg) and then decreases with increased Zn concentration (Fig. 5.2.5(b)). It was found to be 34 Am^2/kg for x = 0.8 sample. Such a small rise at lower dopant concentration could be either due to the Zn^{2+} ions or structural effects. However, for the samples with higher concentrations of Zn ($x \geq 0.2$), the continuous decrease in the M_S values may either be due to the occupancy of Zn^{2+} ions at octahedral sites or due to the canting of moments at B-sites[74,75]. The earlier reports on Zn substitution in magnetite suggest the preference for occupancy of Zn^{2+} ions at tetrahedral sites only. Hence, the effect of canting of moments at B-site could be one of the major reasons. The M_S values may also decrease if some percentage of Fe^{2+} ions also occupies the tetrahedral site. This has been confirmed from Mössbauer spectroscopy which is discussed latter. Nevertheless, the observed M_S values for the sample reported here were less as compared to the earlier reported values[75]. This could be due to the ultrafine size (3-10 nm) of the particles and associated magnetic dead layer on their surface. For such a fine particles, materials should have behaved as a superparamagnet i.e. H_C and M_r values should have been zero. In contrast, the materials exhibited hysteresis loop and the H_C and M_r had integer values (Fig. 5.2.5 b). This suggests that the samples had both ferrimagnetic and superparamagnetic components together. With increased Zn-concentration, H_C values found to be increasing continuously as shown in Fig.5.2.5 (b). Nevertheless, the variation in the H_C value was less. In contrast, the M_r value initially decreased then rose to maxima and finally decreased with increased Zn concentration (Fig. 5.2.5 b). The magnetization vs. temperature curves for $Zn_xFe_{3-x}O_4$ samples at 10 mT are shown in Fig. 5.2.5 (c). The curves indicate that all samples had their T_C above 125 °C).

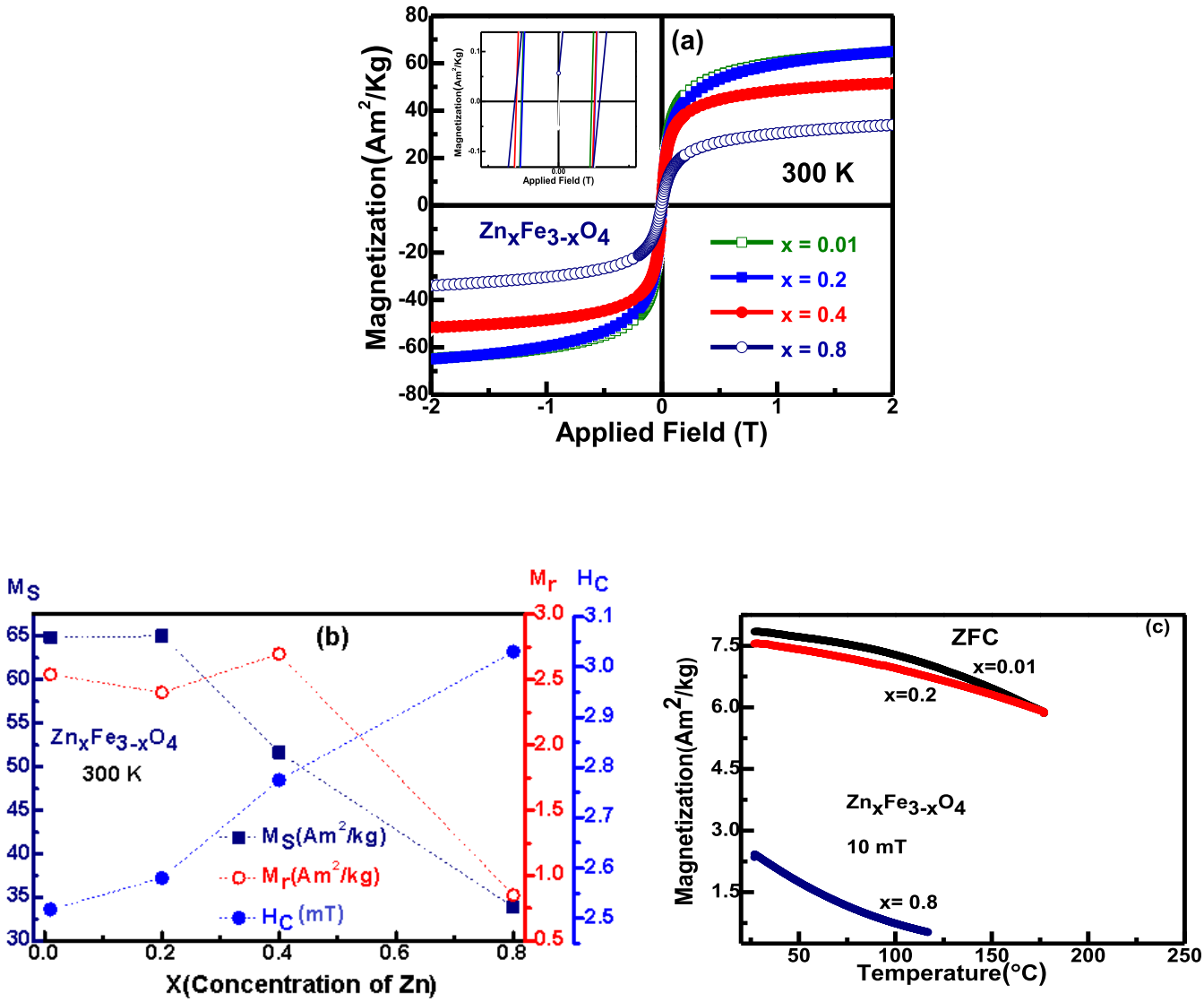

Fig. 5.2.5: (a) Magnetization vs. magnetic field curves at RT and ±2.0 T (b) variation of M_S, M_r and H_C values and (c) *Mvs*. *T* curves at 10 mT for $Zn_xFe_{3-x}O_4$ ($0.01 \leq x \leq 0.8$) samples.

5.2.5. Mössbauer spectroscopy study

To understand further about the variation in the magnetic nature of Fe_3O_4 nanoparticles with Zn substitution, the Mössbauer spectra were recorded at ambient temperature for x = 0.01, 0.07, 0.4 and 0.8 samples and are shown in Fig. 5.2.6. Their respective values for hyperfine field (B_{HF}), isomer shift (δ), quadrupole splitting (Δ), inner line width (Γ) and relative areas (R_A) are listed in table 5.2.2. For $Zn_{0.01}Fe_{2.99}O_4$ sample, the spectrum was fitted with three sextets, out of which two (A and B) represent for tetrahedral and octahedral sites, respectively and third sextet C is due to the shorter spin relaxation time indicates the superparamagnetic nature of nanoparticles (Fig. 5.2.6)[69].

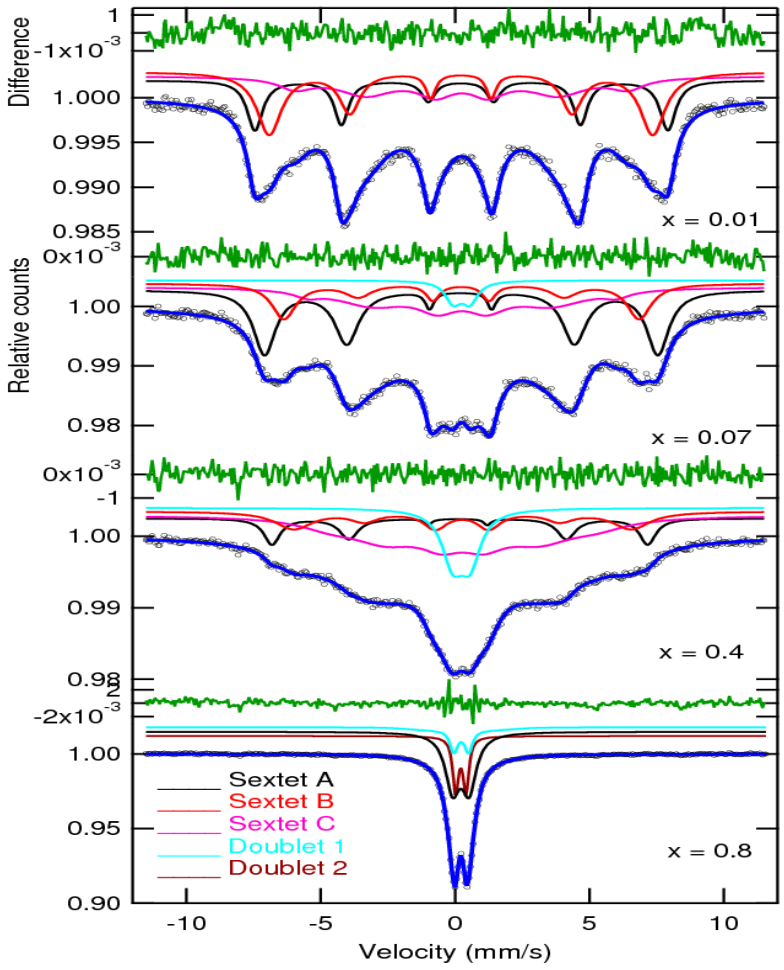

Fig. 5.2.6: Mössbauer spectra of $Zn_xFe_{3-x}O_4$samples (x = 0.01, 0.07, 0.4 and 0.8)

The B_{HF} at the two sites were less than the bulk values due to the submicron sized particles (Fig. 5.2.7 a). Similar decreased values of B_{HF}, were also observed for Hf or Al substituted magnetite samples (chapters 3 and 4) . Further, both the sextets were found to be symmetric and the isomer shifts values were also nearly equal (Fig. 5.2.6 and 5.2.7 b, Table 5.2.2). This happens only if Fe^{2+} ions are present at both the sites. Thus, it strengthens the belief that the occupancy of Fe^{2+} ions in the present samples reduces the M_S value (5.2.5 b). Due to the presence of both ferrimagnetic and superparamagnetic components, the samples have shown smaller values of quadrupole splitting (Fig. 5.2.7 c, Table 5.2.2). The samples with x = 0.07, 0.4 and 0.8 were also fitted with three sextets and a doublet (Fig. 5.2.6). Similar to the first spectra, the two sextets indicate the two vacant sites of spinel structure whereas the other two indicate for superparamagnetic component. The B_{HF} values found to be continuously reducing with increased concentration of Zn which was due to the influence of nonmagnetic ions (Fig. 5.2.7 a, Table 5.2.2). This was in accordance with their M_S values as shown in figure 5.2.5 (b) which also diminished with increased Zn substitutions. The sextets were again symmetric and there IS values were almost similar (Fig. 5.2.6 and 5.2.7 b, Table 5.2.2). Hence, it specifies that Fe^{2+} ions were distributed at both the sites. The values of quadrupole splitting for ferrimagnetic components were nearly 0.01 mms^{-1} whereas it was around 0.62 mms^{-1} for paramagnetic components (Fig. 5.2.7 c). The spectra for x = 0.8 was fitted with one sextets and two doublets (Fig. 5.2.6). The presence of two doublets could be due to increased paramagnetic components in the system due Zn doping. Thus, B_{HF} and M_S values for the sample were too low (Fig. 5.2.5 b and 5.2.7 a, Table 5.2.2). In contrast, the higher splitting values for the samples also indicate the presence of large component of superparamagnetism in the sample.

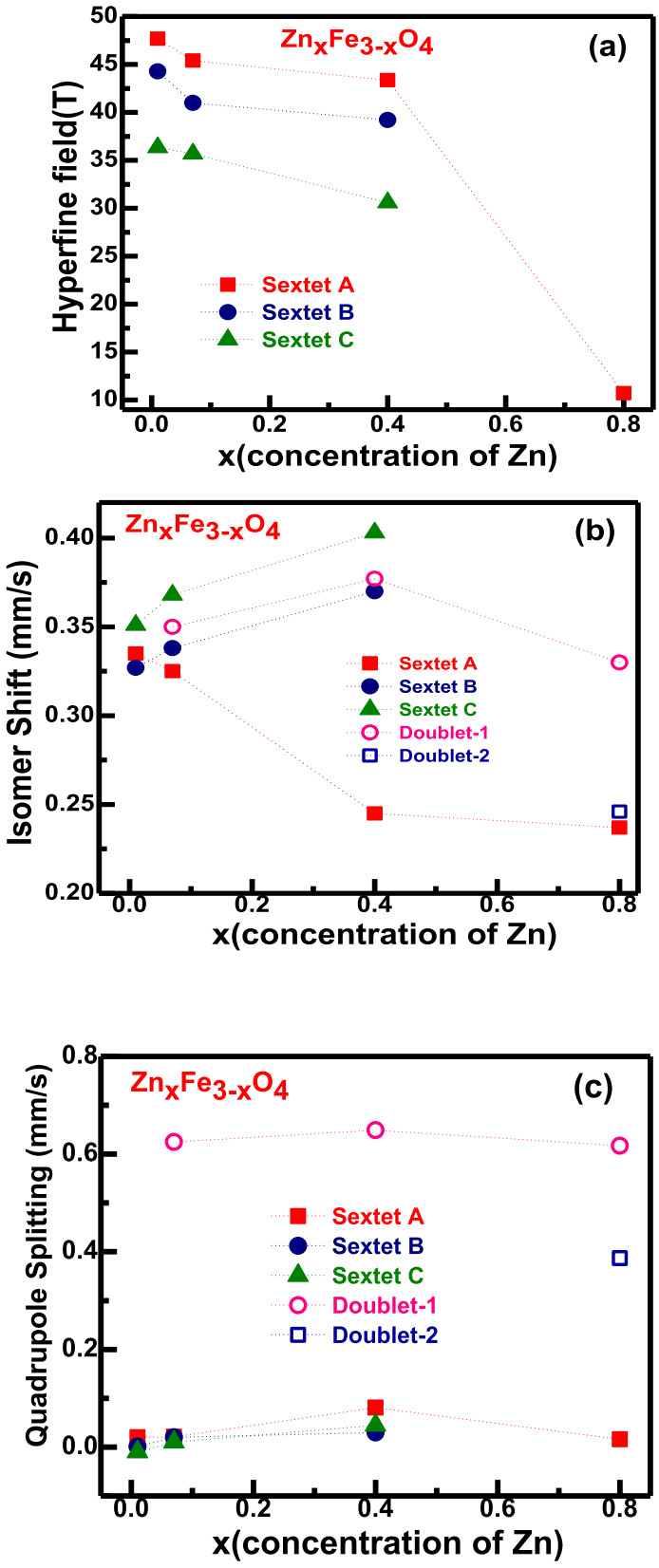

Fig. 5.2.7: Variation in (a)isomer shift (b) Quadrupole splitting and (c) hyperfine field with Zn substitutions in $Zn_xFe_{3-x}O_4$(x = 0.01,0.07, 0.4 and 0.8) samples.

Table 5.2.2:The values of hyperfine field (BHF), isomer shift (δ), quadrupole splitting (Δ), linewidth (Γ) and relative areas (R_A) in percentage of tetrahedral A (Fe^{3+}, Fe^{3+}) and octahedral B sites of (Fe^{3+}, Fe^{2+}) ions for $Zn_xFe_{3-x}O_4$ (x = 0.01,0.07, 0.4 and 0.8) samples derived from Mössbauer spectra recorded at room temperature

Sample Comp. (*x*)	**Iron Sites**	**Hyper. field, (H_{hf}) Tesla (±0.2)**	**Quadrupole splitting, (Δ) mm/s (±0.01)**	**Isomer shift (δ) mm/s (±0.01)**	**Inner Line width (Γ) mm/s (±0.1)**	**Area (R_A) %**	**Fitting quality (χ^2)**
0.01	Sextet A (Fe^{3+}, Fe^{2+})	47.67	0.02	0.335	0.598	19.0	1.131
	Sextet B ($Fe^{3+,}$, Fe^{2+})	44.27	0.001	0.327	0.455	22.7	
	Sextet C (Fe^{3+})	36.34	-0.01	0.351	1.59	58.3	
0.07	Sextet A (Fe^{3+}, Fe^{2+})	45.4	0.021	0.325	0.381	18.4	1.099
	Sextet B (Fe^{3+}, Fe^{2+})	40.99	0.02	0.338	0.63	14.6	
	Sextet C (Fe^{3+})	35.68	0.01	0.368	1.81	65.0	
	Doublet 1 (Fe^{3+})	--	0.625	0.35	0.717	2.0	
0.4	Sextet A (Fe^{3+})	43.36	0.081	0.245	2.3	3.2	0.813
	Sextet B (Fe^{3+}, Fe^{2+})	39.21	0.03	0.37	1.44	16.2	
	Sextet C (Fe^{3+})	30.58	0.045	0.403	2.06	74.6	
	Doublet((Fe^{3+})	--	0.02	0.377	1.06	6.0	
0.8	Sextet A (Fe^{3+}, Fe^{2+})	10.72	0.016	0.34	0.237	24.0	2.49
	Sextet B (Fe^{3+})	--	--	--	--	--	
	Doublet 1	--	0.617	0.33	0.643	66.3	

(Fe^{3+})					
Doublet 2 (Fe^{3+})	--	0.387	0.321	0.246	9.77

Sextet A: Tetrahedral A-site, Sextet B: Octahedral B site, sextet C: Relaxation effect.

5.2.6 Induction heating analysis

The heating abilities for the ferrofluids prepared using nanoparticles of $Zn_xFe_{3-x}O_4$ ($0.01 \leq x \leq 0.8$) were estimated at different combination of amplitudes and frequencies of AC magnetic fields. The temperature vs. time curves for the ferrofluids at a field of amplitude 11 mT and a frequency of 478 kHz are shown in figure 5.2.8 (a). It indicates that the samples with $x = 0.2$ shows continuous rise in the temperature in the presence of field. In contrast, the samples with $x = 0.01$, 0.07, 0.4 and 0.8 show stability of temperature at 45, 42, 36 and 33 °C respectively in the presence of same external magnetic field (figure 5.2.8 a). It is worth to mention here that the M_S values (~33-66 Am^2/kg) for the samples were significant to respond at this magnetic field and show heating behaviour. Further, it has been observed from the M vs. T curves (Fig. 5.2.5 c) that all the $Zn_xFe_{3-x}O_4$ samples had their T_C more than 125°C. Thus, the observed T_S values were not related to the mechanism of transformation of ferrimagnet into paramagnet near T_C. This behaviour was similar to that of the behaviour observed for tetravalent ion (e.g. Zr or Hf) or trivalent (e. g. Al) doped magnetites which are earlier discussed in chapters 3 and 4.

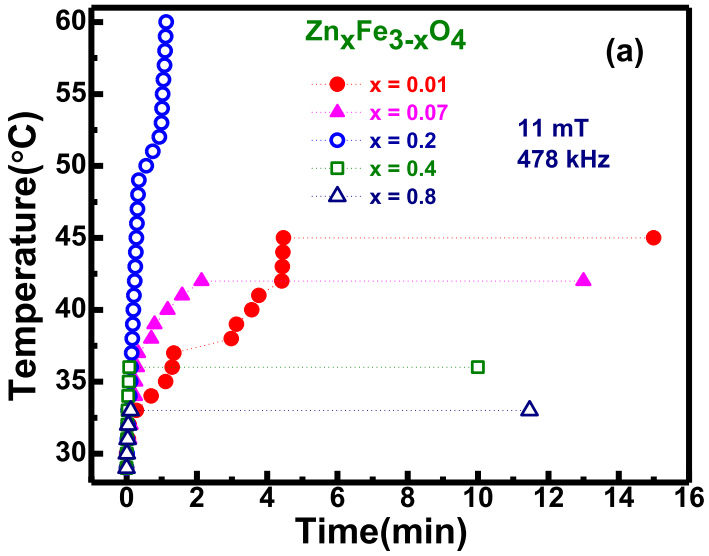

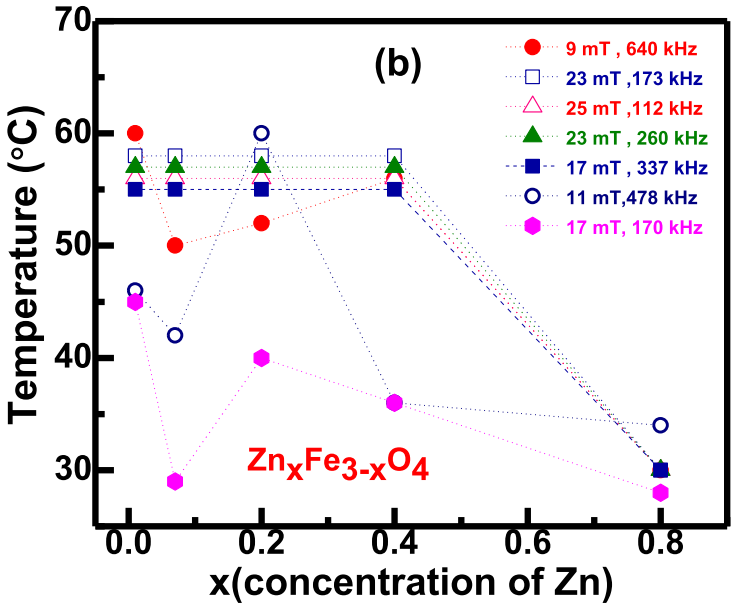

Fig. 5.2.8: (a) Temperature vs. time curves at a field of amplitude of 11 mT and a frequency of 478 kHz and (b) Temperature obtained during magnetic hyperthermia vs. Zn-concentration curves at different fields and frequencies for $Zn_xFe_{3-x}O_4$ ($0.01 \leq x \leq 0.8$) samples.

Further, the ferrofluids were treated at other combinations of amplitudes and frequencies of magnetic fields. The T_S values were also observed at these fields. The temperatures achieved in the presence of various magnetic fields for $Zn_xFe_{3-x}O_4$ samples are shown in Fig. 5.2.8 (b). The temperatures shown at or above 55 °C suggest continuous rise in the temperature during MHT and the other temperature whereas others indicate the stable temperatures (Fig. 5.2.8). As suggested earlier, such magnetic materials, which display stable temperature during magnetic hyperthermia, may be used as an *in-vivo* switch during treatment of animal or humans[66]. The Zn is a cheaper and easily available material as compared to that of Zr, Hf or Ce which were used earlier by our group. Further, Zn-substituted iron oxide nanoparticles have shown better biocompatibility than that of other substituted iron oxides[77].The Food and Drug Administration has also suggested a

permissible daily intake dose for Zn could be up to 15mg/day for human which is relatively higher[78]. Thus, $Zn_xFe_{3-x}O_4$ could be a better option for several bioapplications (e. g. magnetic hyperthermia treatment, thernostic, drug delivery etc.) than that of other tetravalent ions substituted iron oxides.

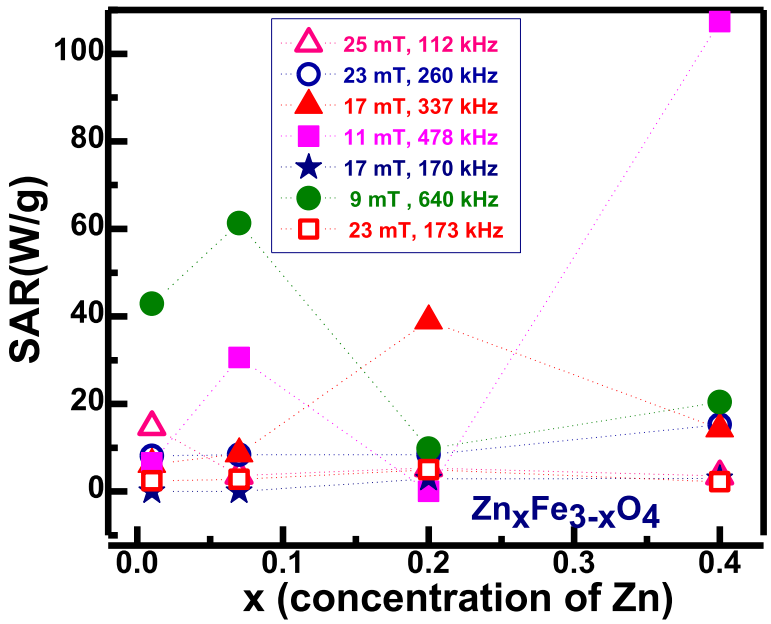

Fig. 5.2.9: The SAR values vs. Zn substitution of $Zn_xFe_{3-x}O_4$ ($0.01 \leq x \leq 0.8$) samples at different frequencies and fields.

The SAR values for $Zn_xFe_{3-x}O_4$ based ferrofluids at various magnetic fields were determined using formula (1) and the values are shown in figure 5.2.9. The highest value of SAR was observed at 11 mT and 478 kHz for the sample with x = 0.4. The SAR values suggest that it also depend on other factors than the M_S values of the MNPs. It has also been observed that the SAR values were more at the fields having higher frequencies e.g. 23 mT, 173 and 260 kHz or 17 mT, 170 and 337 kHz (figure 5.2.9). This was in accordance to the earlier observations where frequency of the AC magnetic field was found as an essential factor during magnetic hyperthermia [42-47].

Further, the SAR values also depends on the amount, type, morphology, polydispersity of the MNPs, physical and chemical natures of the carrier fluid, types of coatings etc. [42,52,71,72].

5.4 Conclusions

$Zn_xFe_{3-x}O_4$ ($0.01 \leq x \leq 0.8$) samples were synthesized using a well-established, simple and one-step microwave refluxing technique. All the samples displayed spinel type structure and a continuous increase in the lattice parameter value was observed with increased Zn content. The size of the particles was found to be between 3 - 11 nm from TEM analysis. The XPS analysis suggests the presence of Fe^{2+}, Fe^{3+} and Zn^{2+} ions in the sample. Due to the occupancy of $Zn^{2+}$and Fe^{2+}ions at tetrahedral sites of spinel structure, the M_S value initially rises slightly and then decreases with increased Zn content. The presence of both ferrimagnetic and superparamagnetic component was suggested from hysteresis loops and Mössbauer spectra. Like, tetravalent or trivalent substituted magnetites, Zn substituted samples also displayed AC field dependent controlled heating during magnetic hyperthermia.